Communications

Compact UWB Antenna With Multiple Band-Notches for WiMAX and WLAN

Ming-Chun Tang, Shaoqiu Xiao, Tianwei Deng, Duo Wang, Jian Guan, Bingzhong Wang, and Guang-Ding Ge

***Abstract*—In order to prevent interference problem due to existing nearby communication systems within the UWB operating frequency, a compact triple band-notch UWB antenna is presented in this communication. This antenna, designed for the rejection of interference with Worldwide Interoperability for Microwave Access (WiMAX), lower and upper wireless local area networks (WLANs) covering 3.3–3.6 GHz, 5.15–5.35 GHz and 5.725–5.825 GHz, provides three notched bands by only one structure with simple design. Based on simulation and measurement, it shows that the proposed antenna can guarantee a wide bandwidth from 3.03 to 11.4 GHz with triple unwanted band-notches successfully.**

***Index Terms*—Complementary co-directional SRR, triple notched bands, UWB antenna.**

I. Introduction

UWB technology has gained a lot of popularity among researchers and wireless industries after the FCC permitted its civil application within the frequency band from 3.1 to 10.6 GHz [1]. With its rapid growth, the ever developing UWB systems raise their demand for compact and low-cost antennas with omnidirectional radiation patterns [2]–[6]. Given the challenges encountered in the UWB antenna design, such as the system interferences, it necessitates the rejection of interference with some narrow bands for UWB applications in other communication systems, for example, the existing WiMAX and WLAN covering the 3.3–3.6 GHz, 5.15–5.35 GHz and 5.725–5.825 GHz [7].

Most examples of compact UWB antennas with band notched characteristic to minimize potential interference have been reported recently. Generally, the existing techniques in extensive use can be classified into the following two categories: One method focuses on loading diverse parasitic elements on the antennas, such as strip near patch [8], split ring resonators (SRRs) or stepped impedance resonators (SIRs) near feed line [9], [10] and ring-shaped patch near ground [11]. The other effective method is embedding various slots, such as arc-shaped slot [12], U-shaped slot [13], square-shaped slot [14], pi-shaped slot [15], H-shaped slot [16], fractal slot [17] and complementary edge-coupled SRR- shaped slot [18]. However, these methods unavoidably exhibit some inherent defects in practical applications. The designs for frequency band rejection function bring occupation of too large space on the antenna as well as strong coupling between band-notch structures. Consequently, most reported antennas can only perform one notched band and fail to meet the requirement of avoiding multiple interferences caused by the coexisting systems. Indeed, scarce dual or triple band-notch antennas can be realized only by loading the rejection function designs of different types, different numbers at different spaces. Therefore, to implement those approaches will require too much space and accordingly result in complicated design. Moreover, the strength and width of each notched band, not being suitable for the rejection of bands for other communication systems, exhibit poor performance. As a result, the design of compact antennas with multiple suitable band-notches has become an imperative research area for both the academia and the industry.

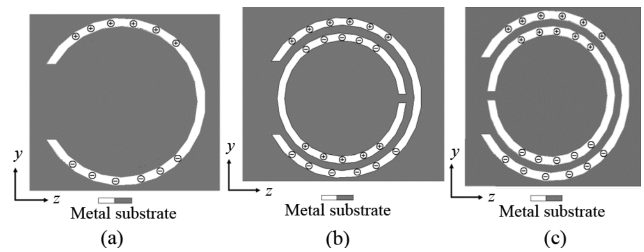

Fig. 1. Topology of different SRRs. (a) Single SRR, (b) Edge-coupled SRR, (c) Co-directional SRR.

Featuring of the multi-frequency signal rejection characteristic, complementary co-directional SRR is promising for UWB antennas to ensure multiple notched bands. With its help in this communication, single, dual and triple notched bands can be easily achieved at such a compact antenna respectively. Especially, the proposed triple band-notch design could provide three suitable notched bands in small enough size. Based on the analysis of radiation, waveform distortion and transmission performance, the proposed antennas demonstrate to be suitable for UWB applications with good rejection of other communication systems interference.

II. Compact UWB Antennas With Single and Dual Band-Notches

A. Different Types of SRR

When time-harmonic external or local magnetic field is applied along the x- axis, it is not difficult to see how the induced current distribution on the electrically small SRR in Fig. 1(a) [19], [20]. The ring, behaving as a circuit driven by an external electromotive force, shows corresponding magnetic resonance and exhibits a band gap above magnetic resonance. According to Babinet's principle [21], when the time-harmonic external or local electric field is applied along the x- axis, complementary SRR could show resonant behavior of the effective permittivity and restrain signal propagation in a narrow band in the vicinity of the resonant frequency. Two types of double-SRR structure are further demonstrated in Figs. 1(b) and 1(c). Similarly, when magnetic field is applied, the SRRs could exhibit corresponding magnetic resonance [19]. In Fig. 1(b) of the traditional edge-coupled SRR, its only one distinct fundamental resonance frequency can be determined by capacitance between the rings due to their different induced charge distributions [20]. In contrast, when the inner ring

Manuscript received March 15, 2010; revised July 04, 2010; accepted October 09, 2010. Date of publication February 10, 2011; date of current version April 06, 2011. This work was supported in part by the Hi-Tech Research and Development Program of China (Grant No. 2009AA01Z231), in part by the National Natural Science Foundation of China (Grant No. 60872034), and in part by the National Defense Pre-Research Foundation of China (Grant No. 08DZ0229, 09DZ0204).

The authors are with the Institute of Applied Physics, University of Electronic Science and Technology of China, Chengdu 610054, China (e-mail: tangmingchunuestc@126.com; xiaoshaoqiu@uestc.edu.cn; aquilauestc@hotmail.com; gp12617@163.com; guanjian1024@hotmail.com; bzwang@uestc.edu.cn; geguangding@uestc.edu.cn).

Digital Object Identifier 10.1109/TAP.2011.2109684

0018-926X/$26.00 © 2011 IEEE

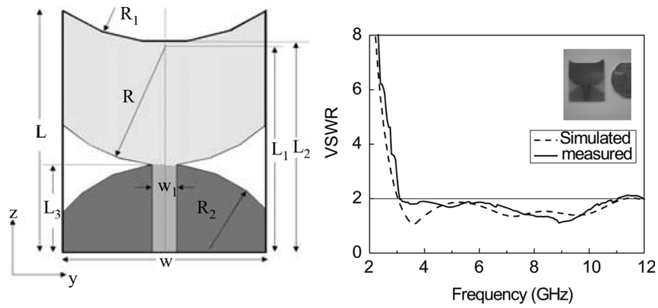

(a) (b)

Fig. 2. Proposed compact UWB antenna. (a) Its sketch with the dimensions: $\mathrm{L} = 30\ \mathrm{mm}$, $\mathrm{L}_1 = 25.65\ \mathrm{mm}$, $\mathrm{L}_2 = 26.95\ \mathrm{mm}$, $\mathrm{L}_3 = 10.65\ \mathrm{mm}$, $\mathrm{W} = 25\ \mathrm{mm}$, $\mathrm{W}_1 = 2.46\ \mathrm{mm}$, $\mathrm{R} = 15.06\ \mathrm{mm}$, $\mathrm{R}_1 = 28\ \mathrm{mm}$, $\mathrm{R}_2 = 16\ \mathrm{mm}$. (b) Voltage standing wave ratio (VSWR) characteristics.

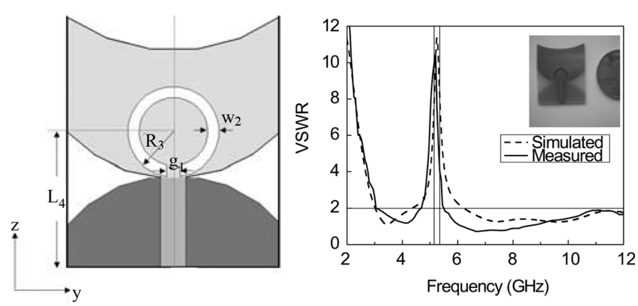

(a) (b)

Fig. 3. Single band-notch UWB antenna. (a) Its sketch with the dimensions: $\mathrm{L}_4 = 13.9\ \mathrm{mm}$, $\mathrm{W}_2 = 0.8\ \mathrm{mm}$, $\mathrm{R}_3 = 3.39\ \mathrm{mm}$, $\mathrm{g}_1 = 1.5\ \mathrm{mm}$. (b) VSWR characteristics.

is placed along the same direction as the outer ring in Fig. 1(c), the capacitance coupling between the rings decreases drastically for their similar induced charge distributions. Thus, the co-directional SRR can exhibit dual distinct fundamental magnetic resonance frequencies for each ring. Analogously, these two corresponding complementary double-SRR structures of Figs. 1(b) and 1(c), out of Babinet's principle [21], could gain electric resonant behaviors and restrain signal propagation. Verified by our simulation study, the complementary edge-coupled SRR could provide only one distinct band gap, while the complementary co-directional SRR, with dual distinct fundamental electric resonance frequencies for dual frequency rejection bands, is of our interest.

B. Compact Planar Antenna Design

Based on the UWB antenna techniques in literatures [2], [8] and [22], a compact planar UWB antenna is presented in Fig. 2(a). In this design, a substrate (FR4) with the permittivity constant $\varepsilon_r = 4.4$ of the height 1.5 mm is selected and a 50 Ω- SMA is connected to the end of the feeding strip and the edge of the ground plane. One measurement of this antenna is carried out with AV3618 Vector Network Analyzer. As shown in Fig. 2(b), the measured results indicate a wide bandwidth 3.05–11.03 GHz with $\mathrm{VSWR} < 2$. This result is in agreement with the simulation (carried out by HFSS [23]) except for a slight deviation at higher frequencies, which can be ignored [2], [20] since the antenna is for use in the 3.1–10.6 GHz band.

C. Compact Antenna With Single Band-Notch

According to the small size of complementary single SRR and its strong signal rejection performance (aforementioned in Section II-A), it is proposed to etch at the patch of the compact UWB antenna to

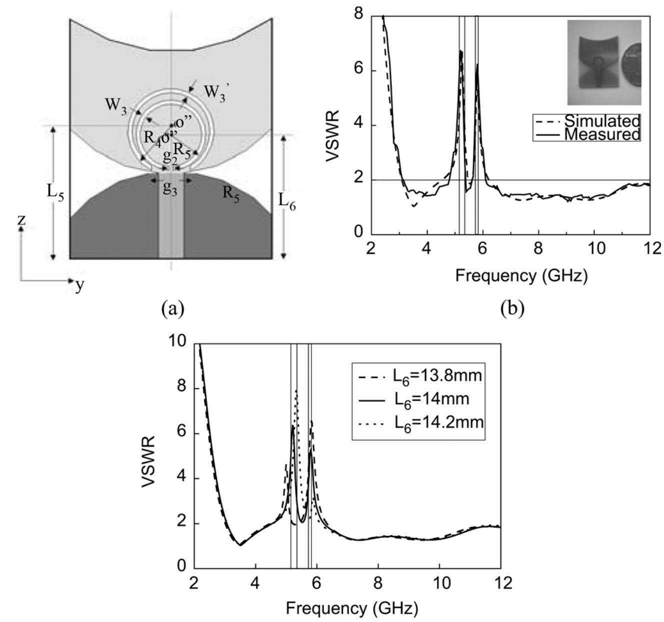

(a) (b)

(c)

Fig. 4. Dual band-notch UWB antenna. (a) Its sketch with the dimensions: $\mathrm{L}_5 = 14.15\ \mathrm{mm}$, $\mathrm{L}_6 = 14\ \mathrm{mm}$, $\mathrm{W}_3 = 0.3\ \mathrm{mm}$, $\mathrm{W}_3' = 0.3\ \mathrm{mm}$, $\mathrm{R}_4 = 3.42\ \mathrm{mm}$, $\mathrm{R}_5 = 2.68\ \mathrm{mm}$, $\mathrm{g}_2 = 0.5\ \mathrm{mm}$, $\mathrm{g}_3 = 3.35\ \mathrm{mm}$. (b) VSWR characteristics. (c) Effect of the complementary co-directional SRR relative positions on the band-notches.

achieve a strong notched band in the operation frequency region in Fig. 3(a). The complementary SRR is arranged in the middle of the patch close to the feeding strip with the gap opposite to the z-axis. As our simulation finds, when the complementary SRR gets closer to the feeding strip, its peak rejection goes higher and rejection band goes wider. Hence, by adjusting the dimensions of complementary SRR, the desired single notched band can be easily achieved.Fig. 3(b) shows the simulated and measured VSWRs versus frequency of the antenna. This UWB antenna could provide sufficiently wide impedance bandwidth $(\mathrm{VSWR} < 2)$ of 3.02–12 GHz and even more at higher frequency and show effective rejection frequency band with high peak rejection centered around 5.25 GHz.

Based on above analysis of the resonance mechanism and our parametric study on the complementary single SRR, the notched frequency can be empirically approximated by

$$f_{notch} = \frac{c}{(L_{inner} + L_{outer}) \cdot \sqrt{\varepsilon_{eff}}} \tag{1}$$

where c is the speed of light and $\varepsilon_{eff} \approx (\varepsilon_r)/2$ the approximated effective dielectric constant; L_{inner} and L_{outer} are the lengths of inner edge and outer edge of complementary SRR, respectively.

D. Compact Antenna With Dual Band-Notches

As aforementioned in Section II-A, the complementary co-directional SRR can show distinct double band gaps due to the weaker mutual coupling between inner and outer rings even the two band gaps are adjacent. Thus, complementary co-directional SRR is selected to obtain adjacent dual notched bands for lower WLAN and upper WLAN here. Parameters of two rings are all designed based on (1). Fig. 4(a) presents the sketch of the dual band-notch UWB antenna. It is noted that the centers of the inner ring and outer ring are not at the same position (the reason will be analyzed in next paragraph). Fig. 4(b) shows its measured and simulated VSWRs versus frequency. The antenna could

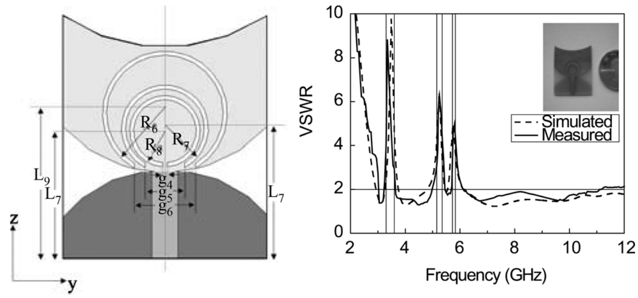

(a) (b)

Fig. 5. Triple band-notch UWB antenna. (a) Its sketch with the dimensions: $\mathrm{L}_7 = 14.2$ mm, $\mathrm{L}_8 = 14.3$ mm, $\mathrm{L}_9 = 15.2$ mm, $\mathrm{R}_6 = 5.2$ mm, $\mathrm{R}_7 = 3.48$ mm, $\mathrm{R}_8 = 2.75$ mm, $\mathrm{g}_4 = 0.3$ mm, $\mathrm{g}_5 = 3.8$ mm, $\mathrm{g}_6 = 6$ mm. (b) VSWR characteristics.

provide sufficiently wide impedance bandwidth $(\mathrm{VSWR} < 2)$ covering 3.08–12 GHz or more with the dual notched bands. Measured dual notched bands are 4.85-5.35 GHz and 5.65–6.08 GHz (where $\mathrm{VSWR} > 2$) respectively, covering lower WLAN and upper WLAN successfully. Therefore, by loading complementary co-directional SRR with different centers, the SRR can provide good dual band-notch performance. Owning to its dual band-notch structure, the complementary co-directional SRR can reduce the design space to achieve dual notched bands in comparison with the complementary edge-coupled SRR [24], [25].

Furthermore, changing the relative position of complementary SRRs is an effective method to adjust each peak rejection and the rejection bandwidth. In Fig. 4(c), the relative positions of the inner and outer complementary rings are discussed. When the inner ring gets close to the feeding strip, its peak rejection goes higher and rejection band goes wider. Meanwhile, for lower notched band, the peak rejection goes lower and rejection band goes narrower. It can be seen from this phenomenon that, when their gaps get closer, the influence on reciprocal resonance strengths becomes more notable.

III. Compact UWB Antenna With Triple Band-Notches

As aforementioned in Section I, the UWB antennas with triple band notches are already presented in [9], [10], [16] and [25]. However, each band-notch structure placed at different positions, takes too much space. Here, a novel structure with three complementary co-directional SRRs is proposed, placing at the superposition to greatly save the space. Considering the weak coupling between the rings in complementary co-directional SRR and the strong notched bands, we further add another complementary ring and investigate a triple band-notch UWB antenna, shown in Fig. 5(a).

The triple band-notch UWB antenna is fabricated and measured. Fig. 5(b) exhibits the measured and simulated VSWRs versus frequency of the triple band-notch antenna. The proposed antenna could provide sufficiently wide impedance bandwidth covering 3.02–11.1 GHz with the triple notched bands, which operate centered around 3.4 GHz, 5.25 GHz, and 5.78 GHz, respectively.

Fig. 6 shows the current distributions at three center notched bands. The dimensions of three complementary SRRs [determined by (1)] are corresponding to three notched bands. When the antenna is working at the center of lower notched band near 3.4 GHz, the outer complementary SRR behaves as a separator in Fig. 6(a), which almost has no relation to the other band-notches. Similarly, the middle complementary SRR operates as a second separator for the center of middle notched band near 5.25 GHz in Fig. 6(b). From Fig. 6(c), the upper notched band near 5.78 GHz is ensured by the inner complementary SRR. Additionally, as a certain current crowded on the ground plane

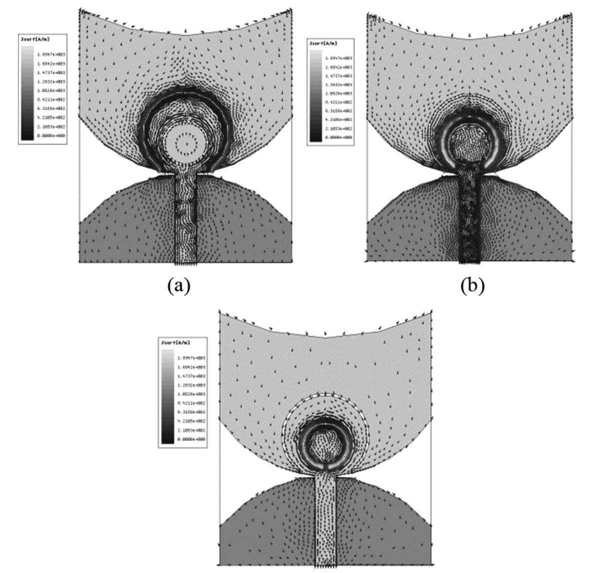

(a) (b) (c)

Fig. 6. The current distribution at (a) 3.4 GHz, (b) 5.25 GHz, (c) 5.78 GHz.

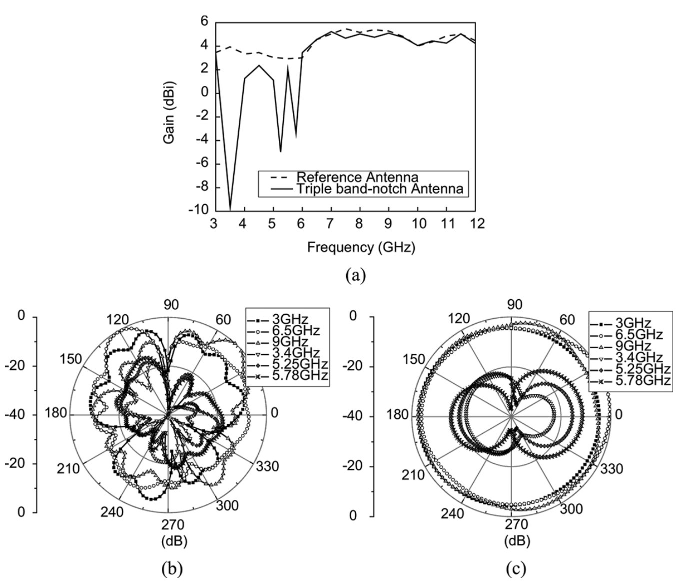

(a)

(b) (c)

Fig. 7. (a) Measured gains of the antennas with and without triple notched bands over the entire UWB frequency band and measured radiation patterns of triple band-notch antenna along (b) xz and (c) xy -cut planes.

near the feed line would affect the antenna performance, we take simulation and find that the dimension of ground plane, especially L_3, has a significant effect on the triple band-notches performance, as well as impedance bandwidth.

The boresight gains at $+x$ direction versus frequency of the reference antenna (without band-notch) and triple band-notch UWB antenna are measured and displayed in Fig. 7(a). It is observed that the average gain of the reference antenna is about 2.9–5.5 dBi over the entire operating band, exhibiting general flat gain performance [26]. When the triple band notches are loaded, the sharp frequency notched characteristic is obtained due to the frequency notched function. The gain reduction is about 13.6 dB at 3.4 GHz, 7.9 dB at 5.25 GHz and 7.6 dB at 5.78 GHz, respectively.

The measured far-field radiation patterns for the triple band-notch UWB antenna at 3 GHz, 6.5 GHz, and 9 GHz are plotted in Figs. 7(b)

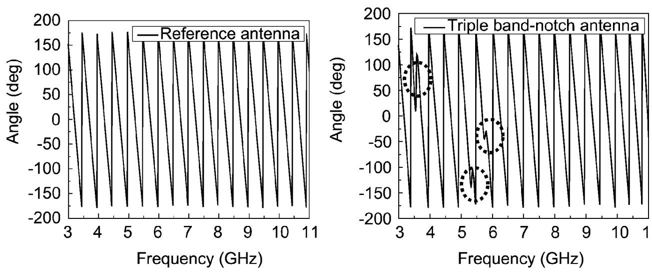

Fig. 8. Phase responses for different identical antenna pairs. (a) Reference antenna in Fig. 2(a). (b) Triple band-notch antenna in Fig. 5(a).

and 7(c). It is seen that the radiation patterns in xy-cut plane (H - plane) are almost omnidirectional and the radiation patterns in xy-cut plane (E-plane) are monopole alike. Clearly, the triple notch UWB antenna has a good radiation performance. When it operates at 3.4 GHz, 5.25 GHz and 5.78 GHz, the gains in the two planes drop significantly, in accordance with the results in Fig. 7(a). It is noted that the radiation pattern at each notched band in H-plane is not omnidirectional because of the dramatically increasing current distribution near three band notches [27], shown in Fig. 6.

To examine the antenna performance in time domain, the phases of transmission response and waveform distortion in the operating frequency region are discussed. Here, a time-domain finite integration technique (CST Microwave Studio) [28] is used to carry out the following simulations. A pair of identical antennas is placed face to face with a distance 0.5 m [9], [26]. It can be seen that the phase response from the original antenna is generally linear in Fig. 8(a). By contrast, the phase response for triple band-notch antenna provided in Fig. 8(b), though witnessing few ripples at notched bands, is also linear.

And then, the normalized source spectrum and the pulses are portrayed in Fig. 9(a) and (b) respectively. The frequency spectrum of modulated Gaussian pulse is chosen corresponding to 3–11 GHz. For original antenna pair, the received signal experiences slight distortion shown in Fig. 9(c), which can be explained by the linear phase response shown in Fig. 8(a) [26]. The received pulse [in Fig. 9(c)] is then transformed into frequency spectrum, as shown in Fig. 9(d). Clearly, we can observe that the operating frequency spectrum also covers UWB region well. Likewise, the similar work is taken to evaluate the triple band-notch antenna performance. Compared with original antenna pair, the triple band-notch antenna pair experiences a little spread in the waveform, indicating that part of the source pulse can not be received as shown in Fig. 9(e) [26]. And in Fig. 9(f), three narrow frequency spectrum bands [corresponding to the results in Figs. 7(a) and 8(b)] takes sharply a great drop in the signal amplitude, reflecting to be hardly transmitted and received by the band-notch antennas. This result in Fig. 9(f) validates that the source pulse, locating within the notched bandwidth, is accurately filtered by the band-notch structure of antenna. Therefore, Fig. 9 illustrates that, the proposed band-notch antenna can restrain the signal transmission within narrow band-notch spectrums effectively and maintain the integrity of signal transmission outside.

Furthermore, the antenna transfer functions ($|S_{21}|$) between pairs of identical antennas are also measured and discussed. In the measurement, the antenna pair, also aligned face to face with a distance 0.5 m, is connected to the two ports of the vector network analyzer indoor [10], [27]. In Fig. 10, the original antenna pair exhibits approximately flat magnitude (-40 to -33 dB) of transfer gain in UWB frequency region. For the triple band-notch antenna pair, the transfer gain remains flat on the whole, except in the notched bands centered around 3.4 GHz, 5.25 GHz, 5.78 GHz, where the magnitudes reduce dramatically by

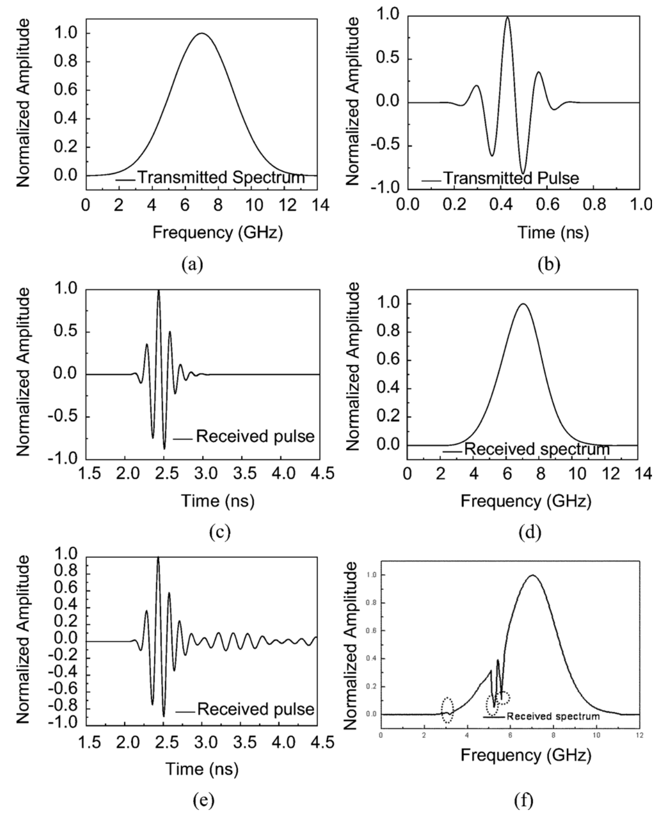

Fig. 9. Transmitted and received waveforms for different identical antenna pairs. (a) Source spectrum. (b) Transmitted waveform. (c) Received waveforms by reference antenna. (d) Received spectrum by reference antenna. (e) Received waveforms by triple band-notch antenna. (f) Received spectrum by triple band-notch antenna.

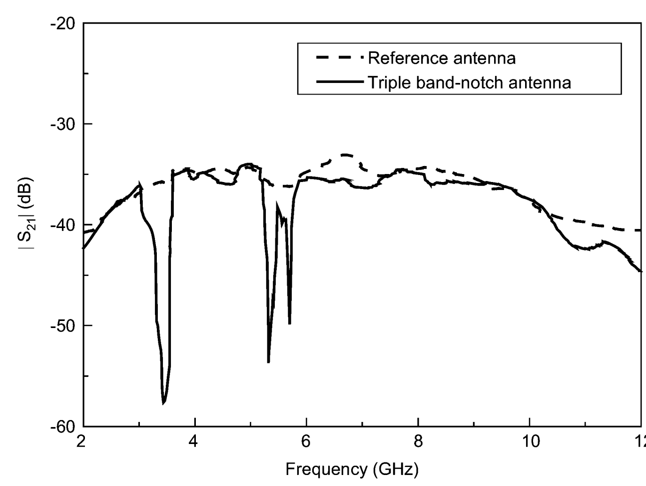

Fig. 10. Experimental results on transfer function of identical antenna pairs.

18–25 dB. Accordingly, the experiment shows agreement with the results in Figs. 7(a) and 9, which further validates its excellent multiple band-notches in UWB communications.

IV. CONCLUSION

We proposed a compact antenna for the rejection of interference with WiMAX and WLAN. Analysis results show that the proposed antenna guarantees a bandwidth wider than the region 3.1–10.6 GHz with unwanted band-notches and keep omnidirectional radiation performance successfully. The performances of the proposed antenna prove it is suitable for UWB applications.

References

[1] *Federal Communications Commission Revision of Part 15 of the Commission's Rules Regarding Ultra-Wideband Transmission System From 3.1 to 10.6 GHz*. Washington, DC: Federal Communications Commission, 2002, pp. 98–153.

[2] Z. N. Chen, T. S. P. See, and X. Qing, "Small printed ultra wideband antenna with reduced ground plane effect," *IEEE Trans. Antennas Propag.*, vol. 55, no. 2, pp. 383–388, Feb. 2007.

[3] M. Gopikrishna, D. D. Krishna, C. K. Anandan, P. Mohanan, and K. Vasudevan, "Design of a compact semi-elliptic monopole slot antenna for UWB systems," *IEEE trans. Antennas propag.*, vol. 57, no. 6, pp. 1834–1837, Jun. 2009.

[4] A. M. Abbosh, "Miniaturization of planar ultra-wideband antenna via corrugation," *IEEE Antennas Wireless Propag. Lett.*, vol. 7, pp. 685–688, 2008.

[5] M. Ojaroudi, G. Kohneshahri, and J. Noory, "Small modified monopole antenna for UWB application," *IET Microw. Antennas Propag.*, vol. 3, no. 5, pp. 863–869, 2009.

[6] M. Ojaroudi, C. Ghobadi, and J. Nourinia, "Small square monopole antenna with inverted T-shaped notch in the ground plane for UWB application," *IEEE Antennas Wireless Propag. Lett.*, vol. 8, pp. 728–731, 2009.

[7] Y. D. Dong, W. Hong, Z. Q. Kuai, C. Yu, Y. Zhang, J. Y. Zhou, and J. Chen, "Development of ultrawideband antenna with multiple band-notched characteristics using half mode substrate integrated waveguide cavity technology," *IEEE Trans. Antennas Propag.*, vol. 57, no. 12, pp. 2894–2902, Dec. 2009.

[8] K. S. Ryu and A. A. Kishk, "UWB antenna with single or dual band-notches for lower WLAN band and upper WLAN band," *IEEE Trans. Antennas Propag.*, vol. 57, no. 12, pp. 3942–3950, Dec. 2009.

[9] Y. Zhang, W. Hong, C. Yu, Z. Kuai, Y. Don, and J. Zhou, "Planar ultra wideband antennas with multiple notched bands based on etched slots on the patch and/or split ring resonators on the feed line," *IEEE Trans. Antennas Propag.*, vol. 56, no. 9, pp. 3063–3068, Sep. 2008.

[10] Y. Zhang, W. Hong, C. Yu, J. Zhou, and Z. Kuai, "Design and implementation of planar ultra-wideband antennas with multiple notched bands based on stepped impedance resonators," *IET Microw. Antennas Propag.*, vol. 3, no. 7, pp. 1051–1059, 2009.

[11] K.-H. Kim and S.-O. Park, "Design of the band-rejected UWB antenna with the ring-shaped parasitic patch," *Microw. Opt. Technol. Lett.*, vol. 48, no. 7, pp. 1310–1313, 2006.

[12] S. J. Hong, J. W. Shin, H. Park, and J. H. Choi, "Analysis of the band-stop techniques for ultrawideband antenna," *Microw. Opt. Technol. Lett.*, vol. 49, pp. 1058–1062, 2007.

[13] W. S. Lee, D. Z. Kim, K. J. Kim, and J. W. Yu, "Wideband planar monopole antennas with dual band-notched characteristics," *IEEE Trans. Microw. Theory Tech.*, vol. 54, pp. 2800–2806, 2006.

[14] S. Hu, H. Chen, C. L. Law, Z. Shen, L. Zui, W. Zhang, and W. Dou, "Backscattering cross section of ultrawideband antennas," *IEEE Antennas Wireless Propag. Lett.*, vol. 6, pp. 70–73, 2007.

[15] Y. L. Zhao, Y. C. Jiao, G. Zhao, L. Zhang, Y. Song, and Z. B. Wong, "Compact planar monopole UWB antenna with band-notched characteristic," *Microw. Opt. Technol. Lett.*, vol. 50, pp. 2656–2658, 2008.

[16] J.-Y. Deng, Y.-Z. Yin, S.-G. Zhou, and Q.-Z. Liu, "Compact ultra-wideband antenna with tri-band notched characteristic," *Electron. Lett.*, vol. 44, no. 21, Oct. 2008.

[17] W. J. Lui, C. H. Cheng, and H. B. Zhu, "Compact frequency notched ultra-wideband fractal printed slot antenna," *IEEE Microw. Wireless Compon. Lett.*, vol. 16, no. 4, pp. 224–226, Apr. 2006.

[18] J. Kim, C. S. Cho, and J. W. Lee, "5.2 GHz notched ultra-wideband antenna using slot-type SRR," *Electron. Lett.*, vol. 42, no. 6, Mar. 2006.

[19] R. Marqués, F. Mesa, J. Martel, and F. Medina, "Comparative analysis of edge- and broadside coupled split ring resonators for metamaterial design-theory and experiments," *IEEE Trans. Antennas Propag.*, vol. 51, no. 10, pp. 2572–2581, Oct. 2003.

[20] T. Koschny, P. Markoš, D. R. Smith, and C. M. Soukoulis, "Resonant and antiresonant frequency dependence of the effective parameters of metamaterials," *Phys. Rev. E*, vol. 68, p. 065602, 2003.

[21] F. Falcone, T. Lopetegi, M. A. G. Laso, J. D. Baena, J. Bonache, M. Beruete, R. Marqués, F. Martín, and M. Sorolla, "Babinet principle applied to the design of metasurfaces and metamaterials," *Phys. Rev. Lett.*, vol. 93, p. 197401, 2004.

[22] Z. N. Chen, N. Yang, Y. X. Guo, and M. Y. W. Chia, "An investigation into measurement of handset antennas," *IEEE Trans. Instrum. Meas.*, vol. 54, pp. 1100–1110, Jun. 2005.

[23] Ansoft High Frequency Structure Simulation (HFSS). ver. 10 Ansoft Corp, 2005.

[24] L. Liu, Y. Z. Yin, C. Jie, J. P. Xiong, and Z. Cui, "A compact printed antenna using slot-type CSRR for 5.2 GHz/5.8 GHz band-notched UWB application," *Microw. Opt. Technol. Lett.*, vol. 50, no. 12, pp. 3239–3242, Dec. 2008.

[25] J. Ding, Z. Lin, Z. Ying, and S. He, "A compact ultra-wideband slot antenna with multiple notch frequency bands," *Microw. Opt. Technol. Lett*, vol. 49, no. 12, pp. 3056–3060, Dec. 2007.

[26] X. N. Low, Z. N. Chen, and T. S. P. See, "A UWB dipole antenna with enhanced impedance and gain performance," *IEEE Trans. Antennas Propag.*, vol. 54, no. 10, pp. 2959–2966, Oct. 2009.

[27] W.-J. Lui, C. Cheng, and H. Zhu, "Improved frequency notched ultra-wideband slot antenna using square ring resonator," *IEEE Trans. Antennas Propag.*, vol. 55, no. 9, pp. 2445–2450, Sep. 2007.

[28] CST Microwave Studio, Computer Simulation Technology (CST), Ver. 4.2 [Online]. Available: www.cst.com

A Wideband Stacked Offset Microstrip Antenna With Improved Gain and Low Cross Polarization

V. P. Sarin, M. S. Nishamol, D. Tony, C. K. Aanandan, P. Mohanan, and K. Vasudevan

***Abstract*—A broadband printed microstrip antenna having $\mathrm{cross\ polarization\ level} > 15\ \mathrm{dB}$ with improved gain in the entire frequency band is presented. Principle of stacking is implemented on a strip loaded slotted broadband patch antenna for enhancing the gain without affecting the broadband impedance matching characteristics and offsetting the position of the upper patch excites a lower resonance which enhances the bandwidth further. The antenna has a dimension of $42 \times 55 \times 4.8\ \mathrm{mm}^3$ when printed on a substrate of dielectric constant 4.2 and has a 2:1 VSWR bandwidth of 34.9%. The antenna exhibits a peak gain of 8.07 dBi and a good front to back ratio better than 12 dB is observed throughout the entire operating band. Simulated and experimental reflection characteristics of the antenna with and without stacking along with offset variation studies, radiation patterns and gain of the final antenna are presented.**

***Index Terms*—Broadband microstrip antenna, gain, offset, stacking.**

I. Introduction

The United States Federal Communication Commission (FCC) has allocated new frequency bands in the 5–6 GHz range under the unlicensed National Information Infrastructure (U-NII) for high speed WLAN. Also European Telecommunications Standards Institute (ETSI) has dedicated a 150 MHz band from 5.15–5.35 GHz for WLAN applications. Although most WLAN applications incorporate

Manuscript received May 06, 2010; revised July 13, 2010; accepted August 11, 2010. Date of publication January 31, 2011; date of current version April 06, 2011. This work was supported in part by the University Grants Commission (UGC), Government of India and Department of Science and Technology (DST), Government of India.

The authors are with Centre for Research in Electromagnetics and Antennas (CREMA), Department of Electronics, Cochin University of Science and Technology, Cochin-22, Kerala, India (e-mail: vasudevan@cusat.ac.in).

Digital Object Identifier 10.1109/TAP.2011.2109362